Key Points:

- Deep learning was applied to multi-band satellite images to detect and quantify *Trichodesmium* surface scums around Australia
- *Trichodesmium* scums were found nearly everywhere around Australia with a seasonality and a cumulative footprint exceeding 4.6 million km^2
- Distribution and seasonality of *Trichodesmium* were driven by temperature, iron-rich dust and black carbon from the mainland bushfires

Trichodesmium Around Australia: A View From Space

Lin Qi[1,2] ⓘ, Menghua Wang[1] ⓘ, Chuanmin Hu[3] ⓘ, Douglas G. Capone[4], Ajit Subramaniam[5] ⓘ, Edward J. Carpenter[6], and Yuyuan Xie[3] ⓘ

[1]NOAA Center for Satellite Applications and Research, College Park, MD, USA, [2]Global Science & Technology Inc., Greenbelt, MD, USA, [3]College of Marine Science, University of South Florida, St. Petersburg, FL, USA, [4]University of Southern California, Los Angeles, CA, USA, [5]Lamont Doherty Earth Observatory, Columbia University, Palisades, NY, USA, [6]Biology Department, Estuary & Ocean Science Center, San Francisco State University, Tiburon, CA, USA

Abstract The cyanobacterium *Trichodesmium* is responsible for approximately half of the ocean's nitrogen input through nitrogen fixation. Although it was first recorded near Australia in the 18th century, the knowledge of where and when large quantity of *Trichodesmium* around Australia could be found is still lacking. Here, using multi-band satellite imagery acquired between 2012 and 2021, we fill this knowledge gap through the use of deep learning, designed to recognize both the spectral shapes of individual pixels and spatial morphology of surface aggregations (scums) of *Trichodesmium*. *Trichodesmium* scums were found nearly everywhere around Australia, with a cumulative footprint (i.e., where the 10-year average density is >0.001‰) exceeding 4.6 million km^2. Strong seasonality was found, with peak months between September and November. Furthermore, temperature, iron-rich dust and black carbon aerosols, with the latter being a result of frequent bushfires, play major roles in determining the spatial distributions and seasonality of *Trichodesmium*.

Plain Language Summary Responsible for half of the ocean's nitrogen input through nitrogen fixation, the saltwater cyanobacterium *Trichodesmium* is ubiquitous in global tropical and subtropical oceans but particularly abundant around Australia. However, although the earliest report goes back to the 18th century, the knowledge of where and when large quantities of *Trichodesmium* can be found around Australia is still incomplete. Based on satellite imagery and deep learning, we quantified relative abundance of *Trichodesmium* around Australia for the period of 2012–2021. Surface aggregations of *Trichodesmium* were found almost everywhere except the southern coast, with a cumulative footprint exceeding 4.6 million km^2. Strong seasonality was found, with peak months between September and November. The spatial distributions and seasonality were found to correlate well with water temperature, iron-rich dust from Australian desert, and black carbon aerosols from frequent bushfires. With the projected ocean warming in the coming century, *Trichodesmium* may expand further south, making the cumulative footprint even larger.

1. Introduction

Trichodesmium is a filamentous cyanobacteria, with *Trichodesmium erythraeum* and *Trichodesmium thiebautii* being the most reported species in the open ocean (Carpenter & Capone, 1992). With abundant gas vesicles, *Trichodesmium* cells can often form buoyant colonies on the surface that appear yellowish or brownish, thus often called sea sawdust (Walsby, 1992). *Trichodesmium* plays a critical role in the ocean's nitrogen cycle, as it is able to fix nitrogen (N_2) to ammonia (NH_4^+) that can be used by itself and other phytoplankton (Capone et al., 1997, 2005; Carpenter & Capone, 1992). On the global scale, *Trichodesmium* can provide about 80 Tg of new nitrogen per year (Capone et al., 1997), representing ∼50% of the total new nitrogen demand in oligotrophic oceans (Capone et al., 2005; Karl et al., 1997). *Trichodesmium* has been reported in oligotrophic oceans, particularly in tropical and subtropical regions where nitrate is scarce. *Trichodesmium* requires iron (Fe) to grow and fix nitrogen (Kustka et al., 2003; Rueter et al., 1992), and both laboratory and field studies showed immediate biomass increases with additional Fe supplies (Lenes et al., 2001; Tzubari et al., 2018).

To date, despite numerous observational and modeling studies at both local and global scales (Blondeau-Patissier et al., 2018; Capone et al., 1997; Davies et al., 2020; Delmont, 2021; M. Furnas, 1992; M. J. Furnas & Carpenter, 2016; Gower et al., 2014; Hu et al., 2010; Karlusich et al., 2021; Y. W. Luo et al., 2012; L. McKinna, 2015; Monteiro et al., 2010; Qi & Hu, 2021; Subramaniam & Carpenter, 1994; Tang & Cassar, 2019; Westberry & Siegel, 2006), the global distributions of *Trichodesmium* are still unclear. Even in waters around

Australia, where *Trichodesmium* was first reported in the 18th century (M. Furnas, 1992), a thorough knowledge of *Trichodesmium* distributions is still lacking.

There have been long-term monitoring programs to measure *Trichodesmium* around Australia. One such program is the Australia's Integrated Marine Observing System (IMOS, https://imos.org.au/; Eriksen et al., 2019). However, these programs are focused on individual sampling sites. Satellite remote sensing has also been used to map *Trichodesmium* surface scums (i.e., surface layer with high concentrations of cells and/or colonies to result in elevated reflectance in the near-infrared wavelengths, see Qi et al., 2018) (see summary in Table S1 and Figure S1 in Supporting Information S1), with the assumption that surface scums can serve as a proxy to represent abundance. Yet these remote sensing studies are either case studies or focused on selected regions (e.g., the Great Barrier Reef or GBR, Blondeau-Patissier et al., 2018; L. McKinna, 2015), thus not being able to provide information on all coastal waters around Australia, especially on where and why *Trichodesmium* blooms occur regularly there.

Here, based on the Visible Infrared Imaging Radiometer Suite (VIIRS) satellite observations and a computer deep learning (DL) model, we develop monthly maps of *Trichodesmium* scum density for a 10-year period between 2012 and 2021 (see Figures S2–S6 and Table S2 for methodology in Supporting Information S1). We analyze the spatial and temporal distributions changes of *Trichodesmium* as well as possible factors leading to such distributions, including atmospheric dust, black carbon (BC) aerosols, water temperature, winds, and ocean currents. We hypothesize that dust and BC are the two primary factors in determining the spatial distributions and seasonality of *Trichodesmium* around Australia.

2. Data and Method

The study around Australia (8°S–40°S and 110°E−160°E, Figure 1a) was based on data collected by VIIRS, the Ocean and Land Color Instruments (OLCI), and the Hyperspectral Imager for the Coastal Ocean (HICO). VIIRS was used to develop time-series of *Trichodesmium* density maps, while limited OLCI and HICO data were used to perform spectral discrimination analysis to verify whether the observed image features were due to *Trichodesmium* or something else. Briefly, for each VIIRS image, pixels containing *Trichodesmium* were first delineated using a DL model (specifically, Res-UNet, see application of the same approach to extract *Sargassum* image features from multi-band imagery over the Atlantic Ocean in Hu et al. (2023)). The DL model relies not only on the reflectance spectral shapes of individual pixels, but also on the spatial context of each pixel, and can be re-trained to improve detection accuracy through minimizing false-positive and false-negative detections, therefore showing better performance over other index-based models (e.g., the alternative floating algae index (AFAI)-based model, Hu et al., 2023). Once *Trichodesmium* features are detected from individual images, a spectral unmixing scheme was used to determine the sub-pixel proportion of *Trichodesmium* (0%–100% within a pixel), and multiple images were used to compose monthly and annual maps. Here, the detected *Trichodesmium* image features refer to surface scums as opposed to cells or colonies suspended in water. The scums show distinctive pigment features in their reflectance spectra (Figures S2 and S3 in Supporting Information S1), indicative of active nitrogen and carbon fixation as reported in the Arabian Sea from similar scums (Capone et al., 1998). More details on this method and its validity can be found in Supporting Information S1.

To interpret the observed spatial patterns and temporal changes of *Trichodesmium*, environmental data from different data sources were downloaded and analyzed. These include: daily sea surface temperature (SST), chlorophyll-*a* (Chl-*a*) concentration, wind speed, and sea surface current velocity; monthly mean dust and BC density in the atmosphere, mixed-layer depth (MLD); all-time averages (i.e., climatology) of sea surface nutrient (nitrogen and phosphorous) concentrations. Further details on these data types can be found in Supporting Information S1.

3. Results and Discussion

3.1. *Trichodesmium* Around Australia: Where and When?

The distribution of average surface density of *Trichodesmium* between 2012 and 2021 is shown in Figure 1a, and more detailed climatological monthly and annual distributions can be found in Figures S7 and S8 in Supporting Information S1, respectively. In the study region (8°S–40°S, 110°E−160°E), *Trichodesmium* scums can be observed almost everywhere around Australia except off the southern coast between 32°S and 40°S and
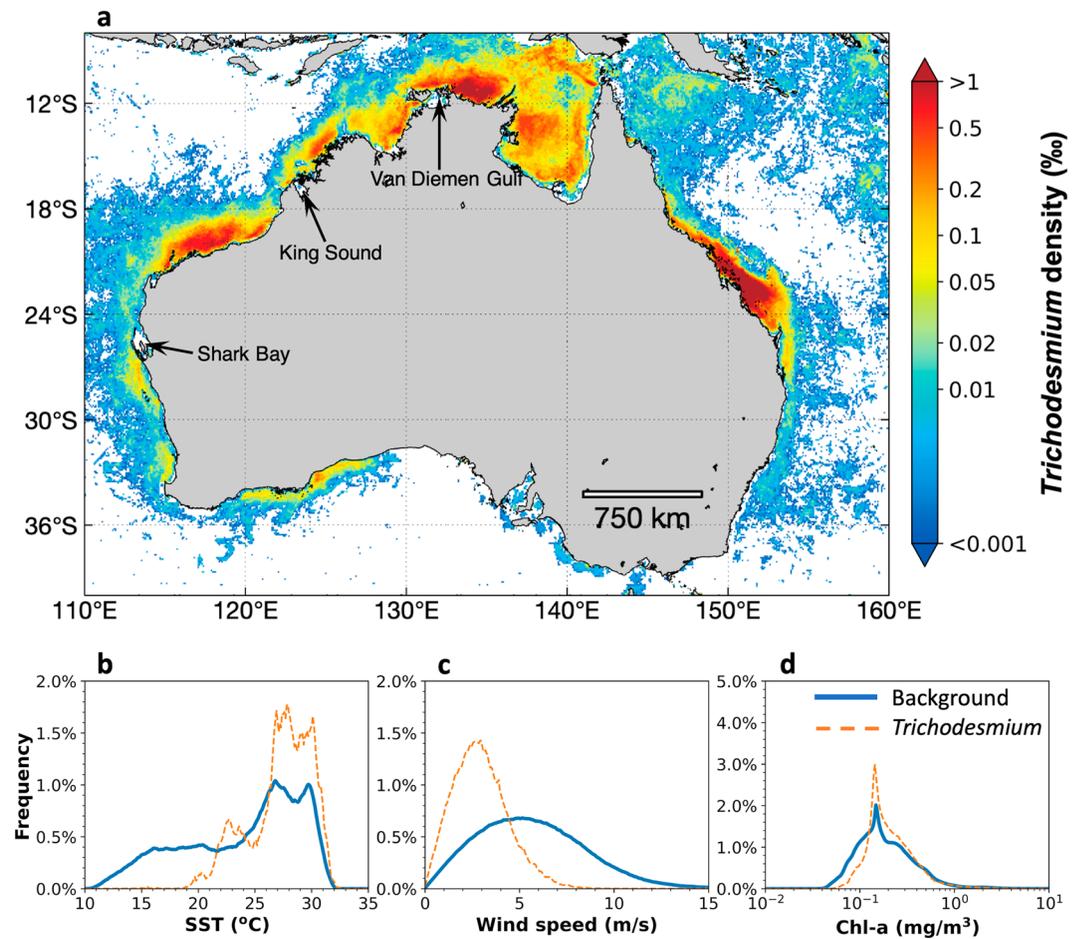
Figure 1. (a) Average surface cover density (in ‰) of floating *Trichodesmium* (i.e., surface scums) around Australia, based on Visible Infrared Imaging Radiometer Suite observations (2012–2021); (b–d) histograms of sea surface temperature, wind speed, and chlorophyll-*a* (Chl-*a*) concentration, respectively, corresponding to occurrence locations of floating *Trichodesmium* (red dashed lines) and their background water of *Tricho*-niche area (i.e., the cumulative footprint area, blue lines). Statistics for tropical/subtropical waters (north of 23.45°S) and temperate waters (south of 23.45°S) are presented in Figure S10 in Supporting Information S1. No *Trichodesmium* scums were found between 40°S and 44°S (including waters around Tasmania), and this area is therefore not included in the map (a). The cumulative footprint, defined as the waters with an average density of >0.001‰ in (a), is ~4.6 million km². Climatological monthly and annual mean distributions of *Trichodesmium* are available in Supporting Information S1.

130°E–150°E. No scums were observed to the south of 40°S (not covered by the map). This is generally in agreement with the model predictions based on field observations (Davies et al., 2020). From Figure 1a, the cumulative footprint of *Trichodesmium*, defined as the waters with a climatological average surface density of >0.001‰, is approximately 4.6 million km². This is equivalent to 60% of Australia's land area.

The distribution is uneven, with most *Trichodesmium* scums found north of ~24°S, for example, in the GBR region, Gulf of Carpentaria, and Arafura Sea. In contrast, in the region south of ~24°S, *Trichodesmium* density is much lower, and no *Trichodesmium* scums were found in the entire 10-year period for the southeast region bounded by 32°S–40°S and 130°E–150°E. Furthermore, the density generally decreased with increasing distance from shore, suggesting possibly land-based nutrient inputs. These spatial patterns are relatively stable from year to year (Figure S8 in Supporting Information S1). The density in this cumulative map is mostly <1‰, suggesting that the appearance of *Trichodesmium* scums is sporadic. This is particularly true for the relatively shallow and dynamic coastal waters such as the Van Diemen Gulf, King Sound, and Shark Bay (Figure 1a). Even though *Trichodesmium* has been reported in these waters, *Trichodesmium* scums were formed much less frequently than in the adjacent, more offshore waters. This is possibly due to the more dynamic water column mixing in these shallow environments (Blondeau-Patissier et al., 2017).
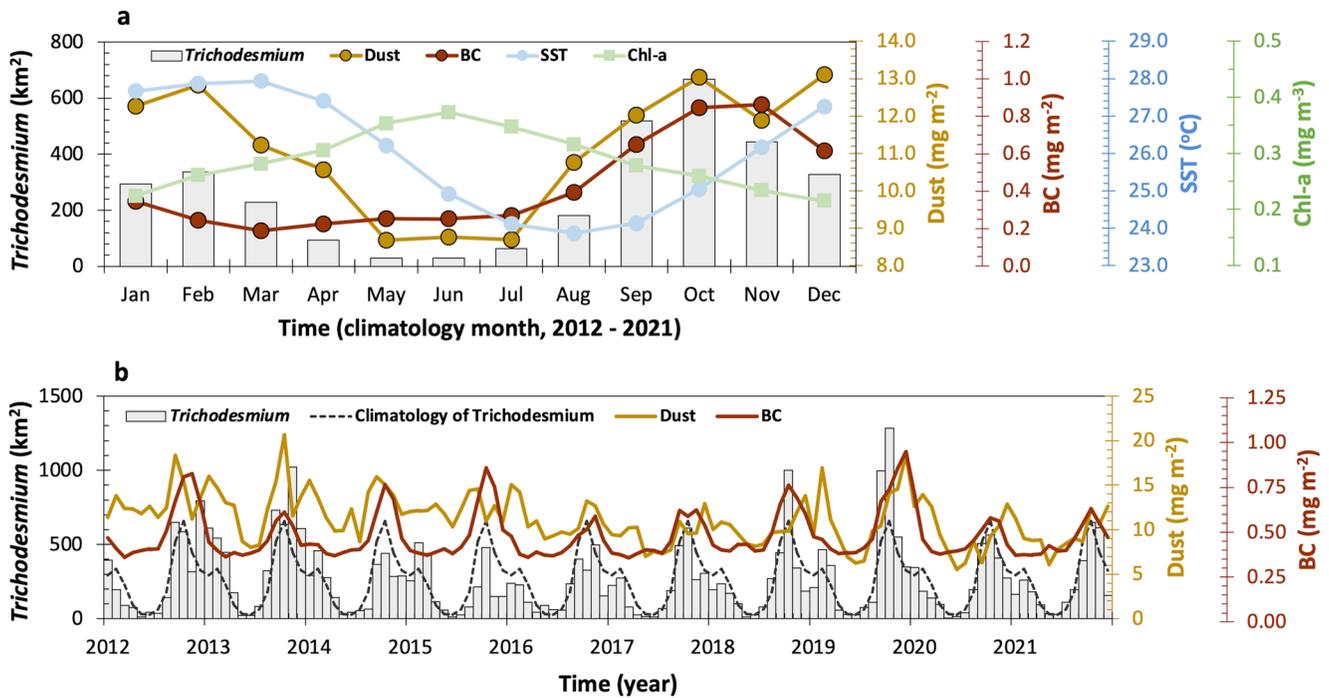
Figure 2. Seasonality (a) and monthly time series (b) of *Trichodusmium* areal coverage between 2012 and 2021. In panel (a), dust, black carbon (BC) aerosols, sea surface temperature, and Chl-*a* derived from the *Tricho*-niche area (i.e., total cumulative footprint area, Figure 1a) are presented. In panel (b), monthly *Trichodesmium* and its corresponding dust and BC from the *Tricho*-niche area are shown, overlaid with the monthly climatological *Trichodesmium*.

Similar to the uneven spatial distributions, *Trichodesmium* was not found equally in all months, but showed a clear seasonality (Figure 2a, Figure S7, and Table S3 in Supporting Information S1) and interannual variability (Figures S8 and S9 in Supporting Information S1) regardless of whether tropical/subtropical and temperate waters were considered together or separately (Figure S10 in Supporting Information S1). The maximum and minimum bloom sizes were found in September–November and May–July, respectively, with a maximum/minimum ratio of about 5. The peak months of *Trichodesmium* blooms can vary slightly from year to year (Figure 2b and Table S3 in Supporting Information S1). For example, in 2014 and 2015, the peak month was February, but there was also a secondary peak in October. In contrast, the months with the minimum bloom size were more stable in different years, mostly between May and July.

3.2. *Trichodesmium* Around Australia: Why?

As per literature and findings prior to this study, *Trichodesmium* scums were not found uniformly in different environments but predominantly in waters within certain temperature and Chl-*a* ranges and under relatively calm conditions (Figures 1b–1d) regardless of whether the entire study region was split into tropical/subtropical (north of 23.45°S) and temperate waters (south of 23.45°S) (Figure S10 in Supporting Information S1). Here, the 10-year cumulative *Trichodesmium* footprint was used as the *Tricho*-niche area, serving as the background water where *Trichodesmium* scums *could* be found (i.e., average 10-year density of *Trichodesmium* >0.001‰ in Figure 1a). SST from *Tricho*-niche waters covered a relatively wide range of 10–32°C, but image pixels containing *Trichodesmium* scums were found in a narrower range of 20–32°C, with the most optimal temperature around 27°C. This temperature range has been reported as the optimal range for *Trichodesmium* growth in the laboratory (Breitbarth et al., 2007). Wind speeds over the *Tricho*-niche waters ranged from 0 to 15 m s^{-1}, but most image pixels containing *Trichodesmium* scums were found at <~6 m s^{-1} (peak frequency ~3.5 m s^{-1}), a result consistent with the findings by Blondeau-Patissier et al. (2018). Likewise, of a relatively wide range of Chl-*a* found from the *Tricho*-niche waters (0.04–2 mg m^{-3}), *Trichodesmium* pixels were found with a narrower Chl-*a* range of 0.07–2 mg m^{-3} and a peak value of ~0.2 mg m^{-3} (Figure 1d). This suggests that, although *Trichodesmium* prefers oligotrophic waters (Capone et al., 1997), it may not survive if the water is extremely poor in nutrients (i.e., Chl-*a* < 0.07 mg m^{-3}). Above this Chl-*a* concentration, *Trichodesmium* may reproduce well and fertilize other

phytoplankton through nitrogen fixation. Here, Chl-*a* is used in a relative sense because of the likely large uncertainties of satellite data products over optically complex coastal waters (Cannizzaro et al., 2013; IOCCG, 2019).

From these results, both the spatial distribution patterns and seasonality of *Trichodesmium* appear to be explained well by the overall nutrient regime and environmental settings around Australia, with some factors playing more important roles than others (Figure 3).

Surrounded by the Indian Ocean and the South Pacific Ocean and being far away from other continents, Australia is the smallest continent on Earth, making it isolated from remote nutrient sources. Thus, local nutrient sources must play a major role in determining the spatial distributions and seasonality of *Trichodesmium*. While average surface nitrate concentration (<0.6 µmol/kg, Voss et al., 2013) suggests oligotrophic conditions, the sea surface nitrate to phosphate ratio (N:P) in surface waters around Australia is ∼2:1 (Figure 3a), much lower than the Redfield ratio of 16:1 required for phytoplankton growth (Lenton & Watson, 2000). Although phosphorus is also a critical nutrient required by *Trichodesmium* (Hynes et al., 2009; Sohm et al., 2008), such a low N/P ratio and oligotrophic condition, together with the optimal temperature range and light availability, provide favorable conditions for *Trichodesmium* to grow as long as another micronutrient, iron, is supplied by certain sources such as riverine input or atmospheric deposition.

With no large river discharging waters to the ocean as compared to many other continents (McMahon & Finlayson, 2003) and with relatively narrow river plume width as compared with shelf width (Sharples et al., 2017), riverine influence on the *Trichodesmium* distributions is expected to be restricted to nearshore waters. Furthermore, compared with other parts of Australia, riverine inputs of dissolved inorganic nitrogen and dissolved inorganic phosphorous to the northwest coast of Australia are lower (Sharples et al., 2017). Thus, the relatively high density of *Trichodesmium* along that part of coast must be driven by factors other than riverine discharge. In the south, riverine flows to the coast are greater in the austral winter (June, July, and August) than in the austral summer (December, January, and February), but there is virtually no *Trichodesmium* found in the south. On the east coast, there are relatively large rivers that discharge to the north and north-east. However, the river flows are extremely seasonal and have high interannual variability, dominated by large flood events in the wet season (October to May in the north) (Warfe et al., 2011). The seasonality of *Trichodesmium* in these waters (Figure S7 in Supporting Information S1) is out of phase of river flow. Therefore, riverine inputs of local nutrients may be ruled out as being a major factor influencing the large-scale distributions of *Trichodesmium*.

The local nutrient sources appear to be from dust (Figure 3b) and BC (Figure 3c). With many large deserts on the Australian continent (∼18% of being permanent deserts and another ∼35% being episodic deserts, Geoscience Australia, 2023), Australia is a major source of dust, with mean dust pathways from the continent to northwest and southeast (De Deckker, 2019) (Figure 3b). Likewise, bushfires or biomass burning are widespread in the northern and southeastern Australia every year because of the dry climate, resulting in high concentrations of BC aerosols with similar southeast-northwest orientation (Figure 3c). Aerosol deposition is an important source of nutrient and iron input to the ocean (Jickells & Moore, 2015; Polyviou et al., 2018; Schulz et al., 2012), and both dust and BC can supply nutrients in the form of C, N, P, and iron to the ocean (Mallet et al., 2017), stimulating growth of *Trichodesmium* and other phytoplankton (Sohm et al., 2011). For example, on the West Florida Shelf, following a Saharan dust event, total dissolved iron concentrations were found to increase by 30–100 folds from the background levels, with *Trichodesmium* concentrations increased by 100 folds (Lenes et al., 2001). In the GBR region, pigment concentration of phytoplankton (likely *Trichodesmium* or other cyanobacteria) was found to increase by 1.5–2 folds after a dust storm event in October 2002 (Shaw et al., 2008). Furthermore, biomass burning may substantially enhance the solubility of mineral dust around Australia, where the soluble iron can be up to ∼12% in the mixed aerosols (Winton et al., 2016). The soluble iron supplies from the atmosphere may help stimulate *Trichodesmium* growth in the oligotrophic waters around Australia.

The distributions of dust and BC do not always correlate with the *Trichodesmium* patterns found in Figure 1a. For example, off southeast Australia, both dust and BC concentrations appear relatively high, yet there is little or no *Trichodesmium* found. Such a disparity may be explained by the strong ocean currents off southeast Australia (>0.5 m s^{-1}, Figure 3d), which can prevent *Trichodesmium* accumulation on the surface and may also impede *Trichodesmium* growth in the water column. In contrast, in similar latitude but off southwest Australia, although wind and SST are similar to those off southeast Australia (Figures 3e and 3f), small amount of *Trichodesmium* scums can still be found due possibly to weaker currents.
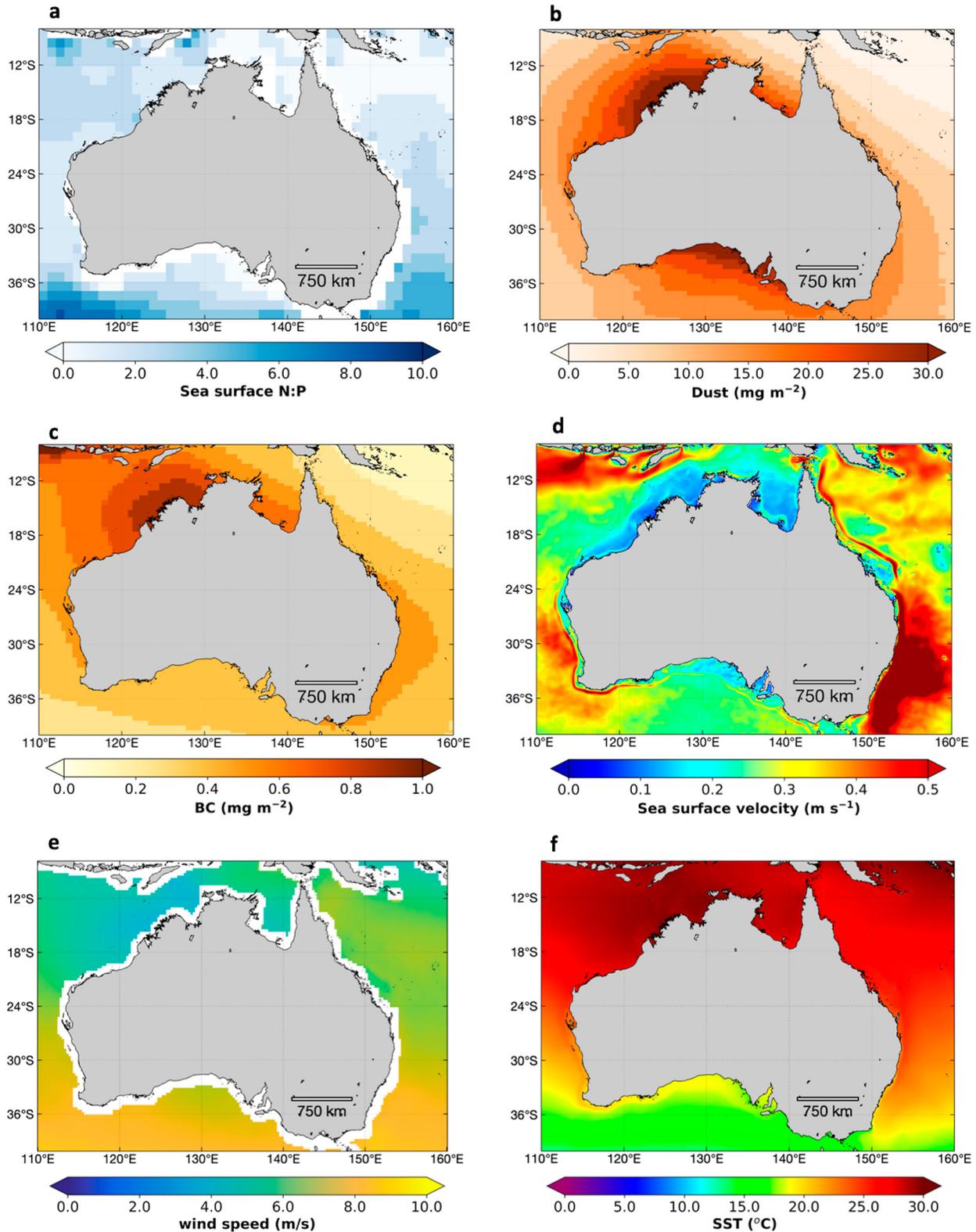
Figure 3. Environmental factors that are relevant to *Trichodesmium* around Australia for (a) surface water nitrate (N) to phosphorus (P) ratio (data source: WOA18), (b) and (c) mean dust and black carbon aerosol concentrations in the atmosphere between 2012 and 2021 (source: M2T1NXAER model), (d) mean surface water velocity during the same period (source: Hybrid Coordinate Ocean Model), (e) and (f) mean wind speed and sea surface temperature during the same period.

In addition to influencing the spatial distributions, dust and BC appear to play an important role in driving the *Trichodesmium* seasonality as well, as all three variables are in phase (Figure 2a) with peak months of September–November and minimum months of May–July. A multi-variate correlation analysis showed strong and statistically significant correction between *Trichodesmium* and the combined variables of BC and dust (Figure S11 in Supporting Information S1), and the regression coefficients for BC and dust are both positive, suggesting their positive influence on *Trichodesmium* growth. Such a high correlation was also found in most high-density locations (Figure S11c in Supporting Information S1). The question is whether this is simply a coincidence as opposed to causality. Because other phytoplankton (through Chl-*a*) shows the opposite phase from dust and BC (i.e., peak Chl-*a* is found between May and July, Figure 2a) and because iron-rich dust and BC are known to stimulate *Trichodesmium* growth, the latter appears to be a logical inference. In particular, the smaller size of the *Tricho*-niche water area between January and March, when dust concentration is nearly as high as that in September–November, may also be explained by the iron mechanism. This is because although dust may contain a greater amount of Fe, most of the Fe in dust aerosols is insoluble and cannot be utilized by phytoplankton (Winton et al., 2016). In contrast, BC contains a higher proportion of soluble Fe, and what's more important is that BC from biomass burning can enhance dusty mineral solubility (Hamilton et al., 2020; Hand et al., 2004; C. Luo et al., 2005; Winton et al., 2016). Thus, the relatively lower BC between January and March may be a reason to explain the lower *Trichodesmium* amount.

The opposite phase between Chl-*a* and dust/BC is perhaps the strongest reason to support the hypothesis that dust and BC can collectively control the seasonality of *Trichodesmium*. From long-term in situ measurements, phytoplankton communities around Australia are dominated by diatoms and dinoflagellates (Eriksen et al., 2019), which are driven by different environmental factors. For example, as in other subtropical oceans such as the Gulf of Mexico (GOM, Muller-Karger et al., 2015) and the South China Sea (SCS, Ji et al., 2018), non-*Trichodesmium* phytoplankton (and their associated Chl-*a*) around Australia may grow fast from nutrient enrichment due to deeper mixing in May–July induced by high winds (Figure S12 in Supporting Information S1). However, because waters around Australia are limited in Fe (Zehr & Capone, 2020), without Fe inputs from the atmosphere, the enhanced nutrients from deep waters would benefit diatoms and dinoflagellates as opposed to *Trichodesmium*. In contrast, *Trichodesmium* may benefit more than diatoms and dinoflagellates with Fe inputs from the atmosphere.

Similar to other cyanobacteria (Paerl & Huisman, 2008) and macroalgae (Qi et al., 2022), *Trichodesmium* also prefers a certain temperature range for optimal growth (Figure 1b), which may explain the overall low abundance in the south than in the north (Figures 1a and 3f). However, temperature may play a less important role in controlling the seasonality of *Trichodesmium* (Figure 2a) because the annual variation of mean SST is 24–28°C, optimal for *Trichodesmium* growth.

The collective role of dust and BC in controlling both spatial distributions (Figure 1a) and seasonality of *Trichodesmium* (Figure 2a) is also reflected in the 10-year monthly time series (Figure 2b). With no significant trend (Mann-Kendall test, $p = 0.72$, Hussain & Mahmud, 2019), inter-annual variations are observed in all three variables, yet a multi-variant regression analysis indicates statistically significant correction ($R = 0.70$, $p < 0.01$) between *Trichodesmium* and combined dust and BC (Figure S11b in Supporting Information S1). In contrast, large-scale climate events such as El Niño and La Niña do not appear to affect the inter-annual changes in *Trichodesmium* of either tropical/subtropical waters or temperate waters, as indicated by the lack of correlation between them (Figure S13 in Supporting Information S1).

Overall, while temperature is an important factor to determine where and when *Trichodesmium* can grow, dust and BC appear to be the other two major factors to drive both spatial and temporal variations of *Trichodesmium* around Australia.

3.3. Impacts of Episodic Events

The dominant roles of dust and BC, as argued above, are supported by episodic events, such as the 2019–2020 bushfire event. This event, from June 2019 to March 2020, is one of the most extensive and long-lasting fires in recent years (Ward et al., 2020). It burned ~46 million acres of land covering forests, farms, and buildings, leading to mortality of 173 people and >1 billion animals (Borchers Arriagada et al., 2020; Ward et al., 2020). About ~715 million tons of CO_2 (195 Tg C) were released into the atmosphere during the fire period (van der Velde et al., 2021), together with nitrogen, phosphorus, and iron depositions into the ocean. The event resulted
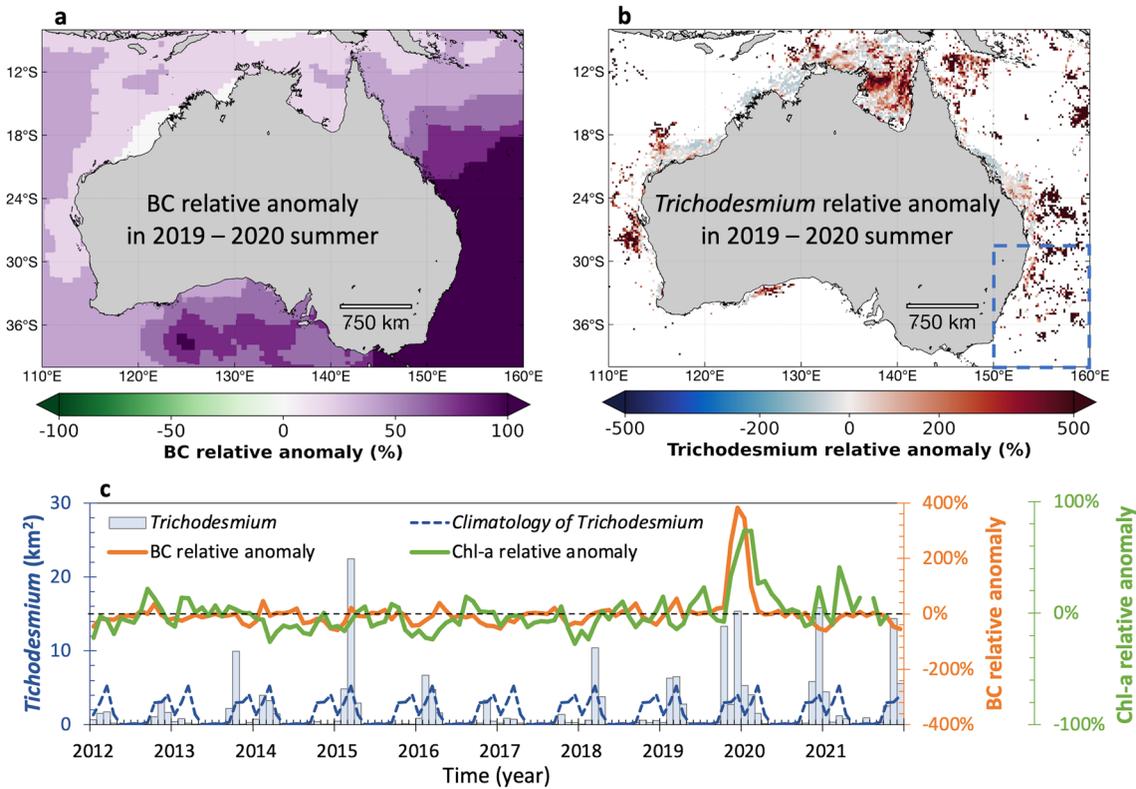
Figure 4. Possible influence of the 2019–2020 Australia bushfire on *Trichodesmium* and Chl-*a* for (a) relative anomaly of black carbon (BC) during the 2019–2020 austral summer season (September 2019–February 2020), (b) relative anomaly of *Trichodesmium* density for the same period, and (c) monthly time series of *Trichodesmium* coverage, relative anomaly of BC, and relative anomaly of Chl-*a* from waters off southeast Australia (blue dashed rectangle in panel (b)). Monthly climatological values of *Trichodesmium* coverage in this region are shown with a dotted dark blue line.

in significantly higher BC around most of Australia, and particularly to the southeast of Australia during the austral summer of 2019–2020 (Figure 4a) as emissions of BC were not uniform (Tang et al., 2021). If the dust/BC hypothesis was true, there would be increased *Trichodesmium* in this region. Indeed, increased *Trichodesmium* was found in this otherwise *Tricho*-poor region (Figure 4b). In other regions where *Trichodesmium* is usually high, increased *Trichodesmium* was also found. For waters off southeast Australia (blue rectangular box in Figure 4b), time-series analysis shows that the timing of the 2019–2020 *Trichodesmium* bloom event and increased Chl-*a* appeared synchronized with the positive BC anomaly (Figure 4c), suggesting a possible causality. In contrast, water temperature and MLD in this region did not show such a correspondence (Figure S14 in Supporting Information S1). In this region, higher-than-usual *Trichodesmium* in this *Tricho*-poor region in three consecutive years after the 2019–2020 bushfire event was abnormal. Using a Mann-Kendal test, no trend in *Trichodesmium* areal coverage was found for the period of 2012–2018 before the bushfire event, yet the increasing trend was statistically significant ($p < 0.05$) when the post-fire years of 2019–2021 were included. To our knowledge, although there are no field data available to explain this pattern, these preliminary results suggest that iron recycling from the ash deposition could be a possible reason. However, this does not necessarily suggest that iron enrichment from bushfire events is the only possible cause of *Trichodesmium* anomalies. For example, in March 2015, an all-time high *Trichodesmium* areal coverage was found, yet there was no positive BC anomaly. The exact reason causing the March 2015 anomaly remains to be investigated.

4. Concluding Remarks

Although recurrent *Trichodesmium* blooms around Australia are well known, especially in the GBR region, the knowledge of where and when blooms occurred has been incomplete until now. The improved knowledge is attributed to the synoptic and frequent satellite measurements to extract *Tricho*-specific signals using a DL technique. These observations fill the knowledge gap for previously undocumented areas along the east, west, and

southern coastlines, suggesting a broader input into the nitrogen cycle of these waters than previously appreciated. Such a knowledge paves the pathway toward the understanding of why *Trichodesmium* around most of Australia is abundant and why strong seasonality is found. For example, while the lack of *Trichodesmium* off southern Australia could be explained by low water temperature, dust and BC aerosols appear to be the other major factors controlling both the spatial distributions and seasonality of *Trichodesmium*, as they collectively serve as a major iron source to stimulate *Trichodesmium* growth. However, much remains to be done to have a better understanding of *Trichodesmium* dynamics around Australia. For example, other than dust and BC aerosols, are there any other iron inputs from ocean circulation or upwelling? With the detailed *Trichodesmium* maps made available through this study, analysis of ocean circulation through hydrodynamic modeling and incorporation of more observational data could help address this question in the near future.

Climate change is a globally pervasive process and Australian coastal waters are not immune to its influences. Upper ocean warming and stratification and acidification are ongoing (Hutchins & Fu, 2017), as well as processes in the terrestrial realm that affect coastal waters such as desertification, changes in coastal runoff and wildfires expansion, in both time and space (Hoegh-Guldberg et al., 2014). How these factors will affect *Trichodesmium* populations (and other diazotrophs) is an area of ongoing research (e.g., Fu et al., 2014), where the findings presented here may serve as the baseline to understand future changes. For example, declining wind stress and increasing SST have been shown in the south and southeast regions of Australia, with the Tasman Sea being the fastest warming region (Duran et al., 2020). Although minimal *Trichodesmium* was found in these regions from the current study, should such wind and SST trends continue in the future, increased *Trichodesmium* would be a consequence, and, likewise, expansion of *Trichodesmium* to higher latitudes could also occur (Breitbarth et al., 2007). With the continuity missions of VIIRS and other satellite missions such as the hyperspectral Plankton, Aerosol, Cloud, ocean Ecosystem (PACE) (https://pace.gsfc.nasa.gov), we expect to extend the data record to future years to understand how *Trichodsmium* around Australia responds to environmental conditions under a changing climate.

Data Availability Statement

The processed data used in this study can be accessed through Mendeley Data: Qi (2023).

References

Blondeau-Patissier, D., Brando, V. E., Lønborg, C., Leahy, S. M., & Dekker, A. G. (2018). Phenology of *Trichodesmium* spp. blooms in the great barrier reef lagoon, Australia, from the ESA-MERIS 10-year mission. *PLoS One*, *13*(12), e0208010. https://doi.org/10.1371/journal.pone.0208010

Blondeau-Patissier, D., Schroeder, T., Clementson, L. A., Brando, V. E., Purcell, D., Ford, P., et al. (2017). Bio-optical properties of two neighboring coastal regions of tropical northern Australia: The Van Diemen Gulf and Darwin Harbour. *Frontiers in Marine Science*, *4*, 114. https://doi.org/10.3389/fmars.2017.00114

Borchers Arriagada, N., Palmer, A. J., Bowman, D. M., Morgan, G. G., Jalaludin, B. B., & Johnston, F. H. (2020). Unprecedented smoke-related health burden associated with the 2019–20 bushfires in eastern Australia. *Medical Journal of Australia*, *213*(6), 282–283. https://doi.org/10.5694/mja2.50545

Breitbarth, E., Oschlies, A., & LaRoche, J. (2007). Physiological constraints on the global distribution of *Trichodesmium*—Effect of temperature on diazotrophy. *Biogeosciences*, *4*(1), 53–61. https://doi.org/10.5194/bg-4-53-2007

Cannizzaro, J., Hu, C., Carder, K. L., Kelble, C. R., Melo, N., Johns, E. M., et al. (2013). On the accuracy of SeaWiFS ocean color data products on the West Florida Shelf. *Journal of Coastal Research*, *29*(6), 1257–1272. https://doi.org/10.2112/JCOASTRES-D-12-00223.1

Capone, D. G., Burns, J. A., Montoya, J. P., Subramaniam, A., Mahaffey, C., Gunderson, T., et al. (2005). Nitrogen fixation by *Trichodesmium* spp.: An important source of new nitrogen to the tropical and subtropical North Atlantic Ocean. *Global Biogeochemical Cycles*, *19*(2), GB2024. https://doi.org/10.1029/2004GB002331

Capone, D. G., Subramaniam, A., Montoya, J. P., Voss, M., Humborg, C., Johansen, A. M., et al. (1998). An extensive bloom of the N2 fixing cyanobacterium *Trichodesmium* in the Eastern Arabian Sea. *Marine Ecology Progress Series*, *172*, 281–292. https://doi.org/10.3354/meps172281

Capone, D. G., Zehr, J. P., Paerl, H. W., Bergman, B., & Carpenter, E. J. (1997). *Trichodesmium*, a globally significant marine cyanobacterium. *Science*, *276*(5316), 1221–1229. https://doi.org/10.1126/science.276.5316.1221

Carpenter, E. J., & Capone, D. G. (1992). Nitrogen fixation in *Trichodesmium* blooms. In *Marine pelagic cyanobacteria: Trichodesmium and other diazotrophs* (pp. 211–217). Springer.

Davies, C., Eriksen, R., & Richardson, A. J. (2020). Spatial and seasonal trends in *Trichodesmium*. In A. J. E. R. M. T. H.-J. I. W. J. R. Richardson (Ed.), *State and trends of Australia's ocean report*. Integrated Marine Observing System (IMOS). https://doi.org/10.26198/5e16abb949e81

De Deckker, P. (2019). An evaluation of Australia as a major source of dust. *Earth-Science Reviews*, *194*, 536–567. https://doi.org/10.1016/j.earscirev.2019.01.008

Delmont, T. O. (2021). Discovery of nondiazotrophic *Trichodesmium* species abundant and widespread in the open ocean. *Proceedings of the National Academy of Sciences*, *118*(46), e2112355118. https://doi.org/10.1073/pnas.2112355118

Duran, E. R., England, M. H., & Spence, P. (2020). Surface ocean warming around Australia driven by interannual variability and long-term trends in Southern Hemisphere westerlies. *Geophysical Research Letters*, *47*(9), e2019GL086605. https://doi.org/10.1029/2019GL086605

Eriksen, R. S., Davies, C. H., Bonham, P., Coman, F. E., Edgar, S., McEnnulty, F. R., et al. (2019). Australia's long-term plankton observations: The integrated marine observing system national reference station network. *Frontiers in Marine Science*, *6*, 161. https://doi.org/10.3389/fmars.2019.00161

Fu, F.-X., Yu, E., Garcia, N. S., Gale, J., Luo, Y., Webb, E. A., & Hutchins, D. A. (2014). Differing responses of marine N2 fixers to warming and consequences for future diazotroph community structure. *Aquatic Microbial Ecology*, *72*(1), 33–46. https://doi.org/10.3354/ame01683

Furnas, M. (1992). Pelagic *Trichodesmium* (=Oscillatoria) in the great barrier reef region. In *Marine pelagic cyanobacteria: Trichodesmium and other Diazotrophs* (pp. 265–272). Springer.

Furnas, M. J., & Carpenter, E. J. (2016). Primary production in the tropical continental shelf seas bordering northern Australia. *Continental Shelf Research*, *129*, 33–48. https://doi.org/10.1016/j.csr.2016.06.006

Geoscience Australia. (2023). Areas of Australian and territory deserts. Retrieved from https://www.ga.gov.au/scientific-topics/national-location-information/landforms/deserts

Gower, J., King, S., & Young, E. (2014). Global remote sensing of *Trichodesmium*. *International Journal of Remote Sensing*, *35*(14), 5459–5466. https://doi.org/10.1080/01431161.2014.926422

Hamilton, D. S., Scanza, R. A., Rathod, S. D., Bond, T. C., Kok, J. F., Li, L., et al. (2020). Recent (1980 to 2015) trends and variability in daily-to-interannual soluble iron deposition from dust, fire, and anthropogenic sources. *Geophysical Research Letters*, *47*(17), e2020GL089688. https://doi.org/10.1029/2020GL089688

Hand, J. L., Mahowald, N. M., Chen, Y., Siefert, R. L., Luo, C., Subramaniam, A., et al. (2004). Estimates of atmospheric-processed soluble iron from observations and a global mineral aerosol model: Biogeochemical implications. *Journal of Geophysical Research*, *109*(D17), D17205. https://doi.org/10.1029/2004JD004574

Hoegh-Guldberg, O., Cai, R., Poloczanska, E. S., Brewer, P. G., Sundby, S., Hilmi, K., et al. (2014). The Ocean. In V. R. Barros, C. B. Field, D. J. Dokken, M. D. Mastrandrea, K. J. Mach, T. E. Bilir, et al. (Eds.), *Climate change 2014: Impacts, adaptation, and vulnerability. Part B: Regional aspects. Contribution of working group II to the fifth assessment report of the intergovernmental panel on climate change* (pp. 1655–1731). Cambridge University Press.

Hu, C., Cannizzaro, J., Carder, K. L., Muller-Karger, F. E., & Hardy, R. (2010). Remote detection of *Trichodesmium* blooms in optically complex coastal waters: Examples with MODIS full-spectral data. *Remote Sensing of Environment*, *114*(9), 2048–2058. https://doi.org/10.1016/j.rse.2010.04.011

Hu, C., Zhang, S., Barnes, B. B., Xie, Y., Wang, M., Cannizzaro, J. P., & English, D. C. (2023). Mapping and quantifying pelagic *Sargassum* in the Atlantic Ocean using multi-band medium-resolution satellite data and deep learning. *Remote Sensing of Environment*, *289*, 113515. https://doi.org/10.1016/j.rse.2023.113515

Hussain, M., & Mahmud, I. (2019). pyMannKendall: A Python package for non parametric Mann Kendall family of trend tests. *Journal of Open Source Software*, *4*(39), 1556. https://doi.org/10.21105/joss.01556

Hutchins, D. A., & Fu, F. (2017). Microorganisms and ocean global change. *Nature Microbiology*, *2*(6), 17058. https://doi.org/10.1038/nmicrobiol.2017.58

Hynes, A. M., Chappell, P. D., Dyhrman, S. T., Doney, S. C., & Webbd, E. A. (2009). Cross-basin comparison of phosphorus stress and nitrogen fixation in *Trichodesmium*. *Limnology & Oceanography*, *54*(5), 1438–1448. https://doi.org/10.4319/lo.2009.54.5.1438

IOCCG. (2019). Uncertainties in ocean colour remote sensing. In F. Mélin (Ed.), *IOCCG report series, no. 18, international ocean colour coordinating group, Dartmouth, Canada*. https://doi.org/10.25607/OBP-696

Ji, C., Zhang, Y., Cheng, Q., Tsou, J., Jiang, T., & Liang, X. S. (2018). Evaluating the impact of sea surface temperature (SST) on spatial distribution of chlorophyll-*a* concentration in the East China Sea. *International Journal of Applied Earth Observation and Geoinformation*, *68*, 252–261. https://doi.org/10.1016/j.jag.2018.01.020

Jickells, T., & Moore, C. M. (2015). The importance of atmospheric deposition for ocean productivity. *Annual Review of Ecology, Evolution, and Systematics*, *46*(1), 481–501. https://doi.org/10.1146/annurev-ecolsys-112414-054118

Karl, D. M., Letelier, R. M., Tupas, L., Dore, J. E., Christian, J. R., & Hebel, D. (1997). The role of nitrogen fixation in biogeochemical cycling in the subtropical north Pacific Ocean. *Nature*, *388*(6642), 533–538. https://doi.org/10.1038/41474

Karlusich, J. J. P., Pelletier, E., Lombard, F., Carsique, M., Dvorak, E., Colin, S., et al. (2021). Global distribution patterns of marine nitrogen-fixers by imaging and molecular methods. *Nature Communications*, *12*(1), 4160. https://doi.org/10.1038/s41467-021-24299-y

Kustka, A. B., Sañudo-Wilhelmy, S. A., Carpenter, E. J., Capone, D., Burns, J., & Sunda, W. G. (2003). Iron requirements for dinitrogen-and ammonium-supported growth in cultures of *Trichodesmium* (IMS 101): Comparison with nitrogen fixation rates and iron: Carbon ratios of field populations. *Limnology & Oceanography*, *48*(5), 1869–1884. https://doi.org/10.4319/lo.2003.48.5.1869

Lenes, J. M., Darrow, B. P., Cattrall, C., Heil, C. A., Callahan, M., Vargo, G. A., et al. (2001). Iron fertilization and the *Trichodesmium* response on the West Florida shelf. *Limnology & Oceanography*, *46*(6), 1261–1277. https://doi.org/10.4319/lo.2001.46.6.1261

Lenton, T. M., & Watson, A. J. (2000). Redfield revisited: 1. Regulation of nitrate, phosphate, and oxygen in the ocean. *Global Biogeochemical Cycles*, *14*(1), 225–248. https://doi.org/10.1029/1999gb900065

Luo, C., Mahowald, N. M., Meskhidze, N., Chen, Y., Siefert, R. L., Baker, A. R., & Johansen, A. M. (2005). Estimation of iron solubility from observations and a global aerosol model. *Journal of Geophysical Research*, *110*(D23), D23307. https://doi.org/10.1029/2005JD006059

Luo, Y.-W., Doney, S. C., Anderson, L. A., Benavides, M., Berman-Frank, I., Bode, A., et al. (2012). Database of diazotrophs in global ocean: Abundance, biomass and nitrogen fixation rates. *Earth System Science Data*, *4*(1), 47–73. https://doi.org/10.5194/essd-4-47-2012

Mallet, M. D., Desservettaz, M. J., Miljevic, B., Milic, A., Ristovski, Z. D., Alroe, J., et al. (2017). Biomass burning emissions in north Australia during the early dry season: An overview of the 2014 SAFIRED campaign. *Atmospheric Chemistry and Physics*, *17*(22), 13681–13697. https://doi.org/10.5194/acp-17-13681-2017

McKinna, L. (2015). Three decades of ocean-color remote-sensing *Trichodesmium* spp. in the World's oceans: A review. *Progress in Oceanography*, *131*, 177–199. https://doi.org/10.1016/j.pocean.2014.12.013

McMahon, T. A., & Finlayson, B. L. (2003). Droughts and anti-droughts: The low flow hydrology of Australian rivers. *Freshwater Biology*, *48*(7), 1147–1160. https://doi.org/10.1046/j.1365-2427.2003.01098.x

Monteiro, F. M., Follows, M. J., & Dutkiewicz, S. (2010). Distribution of diverse nitrogen fixers in the global ocean. *Global Biogeochemical Cycles*, *24*(3), GB3017. https://doi.org/10.1029/2009GB003731

Muller-Karger, F. E., Smith, J. P., Werner, S., Chen, R., Roffer, M., Liu, Y., et al. (2015). Natural variability of surface oceanographic conditions in the offshore Gulf of Mexico. *Progress in Oceanography*, *134*, 54–76. https://doi.org/10.1016/j.pocean.2014.12.007

Paerl, H. W., & Huisman, J. (2008). Blooms like it Hot. *Science*, *320*(5872), 57–58. https://doi.org/10.1126/science.1155398

Polyviou, D., Baylay, A. J., Hitchcock, A., Robidart, J., Moore, C. M., & Bibby, T. S. (2018). Desert dust as a source of iron to the globally important diazotroph *Trichodesmium*. *Frontiers in Microbiology*, *8*. https://doi.org/10.3389/fmicb.2017.02683

Qi, L. (2023). "*Trichodesmium* around Australia: A view from space", V1. https://doi.org/10.17632/f5d72t72b3.1

Qi, L., Hu, C., Barnes, B. B., Lapointe, B. E., Chen, Y., Xie, Y., & Wang, M. (2022). Climate and anthropogenic controls of seaweed expansions in the east China sea and yellow sea. *Geophysical Research Letters*, *49*(19), e2022GL098185. https://doi.org/10.1029/2022GL098185

Qi, L., Hu, C., Mikelsons, K., Wang, M., Lance, V., Sun, S., et al. (2020). In search of floating algae and other organisms in global oceans and lakes. *Remote Sensing of Environment*, *239*, 111659. https://doi.org/10.1016/j.rse.2020.111659

Qi, L., Hu, C., Visser, P. M., & Ma, R. (2018). Diurnal changes of cyanobacteria blooms in Taihu Lake as derived from GOCI observations. *Limnology & Oceanography*, *63*(4), 1711–1726. https://doi.org/10.1002/lno.10802

Rueter, J. G., Hutchins, D. A., Smith, R. W., & Unsworth, N. L. (1992). Iron nutrition of *Trichodesmium*. In *Marine pelagic cyanobacteria: Trichodesmium and other diazotrophs* (pp. 289–306). Springer.

Schulz, M., Prospero, J. M., Baker, A. R., Dentener, F., Ickes, L., Liss, P. S., et al. (2012). Atmospheric transport and deposition of mineral dust to the ocean: Implications for research needs. *Environmental Science & Technology*, *46*(19), 10390–10404. https://doi.org/10.1021/es300073u

Sharples, J., Middelburg, J. J., Fennel, K., & Jickells, T. D. (2017). What proportion of riverine nutrients reaches the open ocean? *Global Biogeochemical Cycles*, *31*(1), 39–58. https://doi.org/10.1002/2016gb005483

Shaw, E. C., Gabric, A. J., & McTainsh, G. H. (2008). Impacts of aeolian dust deposition on phytoplankton dynamics in Queensland coastal waters. *Marine and Freshwater Research*, *59*(11), 951–962. https://doi.org/10.1071/MF08087

Sohm, J. A., Mahaffey, C., & Capone, D. G. (2008). Assessment of relative phosphorus limitation of *Trichodesmium* spp. in the north pacific, north Atlantic, and the north coast of Australia. *Limnology & Oceanography*, *53*(6), 2495–2502. https://doi.org/10.4319/lo.2008.53.6.2495

Sohm, J. A., Webb, E. A., & Capone, D. G. (2011). Emerging patterns of marine nitrogen fixation. *Nature Reviews Microbiology*, *9*(7), 499–508. https://doi.org/10.1038/nrmicro2594

Subramaniam, A., & Carpenter, E. J. (1994). An empirically derived protocol for the detection of blooms of the marine cyanobacterium *Trichodesmium* using CZCS imagery. *International Journal of Remote Sensing*, *15*(8), 1559–1569. https://doi.org/10.1080/01431169408954191

Tang, W., & Cassar, N. (2019). Data-driven modeling of the distribution of diazotrophs in the global ocean. *Geophysical Research Letters*, *46*(21), 12258–12269. https://doi.org/10.1029/2019GL084376

Tang, W., Llort, J., Weis, J., Perron, M. M. G., Basart, S., Li, Z., et al. (2021). Widespread phytoplankton blooms triggered by 2019–2020 Australian wildfires. *Nature*, *597*(7876), 370–375. https://doi.org/10.1038/s41586-021-03805-8

Tzubari, Y., Magnezi, L., Be'er, A., & Berman-Frank, I. (2018). Iron and phosphorus deprivation induce sociality in the marine bloom-forming cyanobacterium *Trichodesmium*. *The ISME Journal*, *12*(7), 1682–1693. https://doi.org/10.1038/s41396-018-0073-5

van der Velde, I. R., van der Werf, G. R., Houweling, S., Maasakkers, J. D., Borsdorff, T., Landgraf, J., et al. (2021). Vast CO_2 release from Australian fires in 2019–2020 constrained by satellite. *Nature*, *597*(7876), 366–369. https://doi.org/10.1038/s41586-021-03712-y

Voss, M., Bange, H. W., Dippner, J. W., Middelburg, J. J., Montoya, J. P., & Ward, B. (2013). The marine nitrogen cycle: Recent discoveries, uncertainties and the potential relevance of climate change. *Philosophical transactions of the Royal Society of London. Series B, Biological sciences*, *368*(1621), 20130121. https://doi.org/10.1098/rstb.2013.0121

Walsby, A. (1992). The gas vesicles and buoyancy of *Trichodesmium*. In *Marine pelagic cyanobacteria: Trichodesmium and other diazotrophs* (pp. 141–161). Springer.

Ward, M., Tulloch, A. I. T., Radford, J. Q., Williams, B. A., Reside, A. E., Macdonald, S. L., et al. (2020). Impact of 2019–2020 mega-fires on Australian fauna habitat. *Nature Ecology & Evolution*, *4*(10), 1321–1326. https://doi.org/10.1038/s41559-020-1251-1

Warfe, D. M., Pettit, N. E., Davies, P. M., Pusey, B. J., Hamilton, S., Kennard, M. J., et al. (2011). The 'wet–dry' in the wet-dry tropics drives river ecosystem structure and processes in northern Australia. *Freshwater Biology*, *56*(11), 2169–2195. https://doi.org/10.1111/j.1365-2427.2011.02660.x

Westberry, T. K., & Siegel, D. A. (2006). Spatial and temporal distribution of *Trichodesmium* blooms in the world's oceans. *Global Biogeochemical Cycles*, *20*(4), GB4016. https://doi.org/10.1029/2005gb002673

Winton, V. H. L., Edwards, R., Bowie, A. R., Keywood, M., Williams, A. G., Chambers, S. D., et al. (2016). Dry season aerosol iron solubility in tropical northern Australia. *Atmospheric Chemistry and Physics*, *16*(19), 12829–12848. https://doi.org/10.5194/acp-16-12829-2016

Zehr, J. P., & Capone, D. G. (2020). Changing perspectives in marine nitrogen fixation. *Science*, *368*(6492), eaay9514. https://doi.org/10.1126/science.aay9514

References From the Supporting Information

Bell, P. R. F. (2021). Analysis of satellite imagery using a simple algorithm supports evidence that *Trichodesmium* supplies a significant new nitrogen load to the GBR lagoon. *Ambio*, *50*(6), 1200–1210. https://doi.org/10.1007/s13280-020-01460-3

Cannizzaro, J. P., Barnes, B. B., Hu, C., Corcoran, A. A., Hubbard, K. A., Muhlbach, E., et al. (2019). Remote detection of cyanobacteria blooms in an optically shallow subtropical lagoonal estuary using MODIS data. *Remote Sensing of Environment*, *231*, 111227. https://doi.org/10.1016/j.rse.2019.111227

Chatterjee, S., & Hadi, A. S. (1986). Influential observations, high leverage points, and outliers in linear regression. *Statistical Science*, *1*(3), 379–393. https://doi.org/10.1214/ss/1177013622

Chin, T. M., Vazquez-Cuervo, J., & Armstrong, E. M. (2017). A multi-scale high-resolution analysis of global sea surface temperature. *Remote Sensing of Environment*, *200*, 154–169. https://doi.org/10.1016/j.rse.2017.07.029

Gao, L., Wang, C., Liu, K., Chen, S., Dong, G., & Su, H. (2022). Extraction of floating raft Aquaculture areas from sentinel-1 SAR images by a Dense residual U-net model with pre-trained Resnet34 as the encoder. *Remote Sensing*, *14*(13), 3003. https://doi.org/10.3390/rs14133003

Hu, C. (2022). Hyperspectral reflectance spectra of floating matters derived from Hyperspectral Imager for the Coastal Ocean (HICO) observations. *Earth System Science Data*, *14*(3), 1183–1192. https://doi.org/10.5194/essd-14-1183-2022

McKinna, L. I. W. (2010). *Optical detection and quantification of Trichodesmium spp. within the Great Barrier Reef* (PhD thesis) (p. 312). James Cook University. Retrieved from https://researchonline.jcu.edu.au/15643/

McKinna, L. I. W., Furnas, M. J., & Ridd, P. V. (2011). A simple, binary classification algorithm for the detection of *Trichodesmium* spp. within the Great Barrier Reef using MODIS imagery. *Limnology and Oceanography: Methods*, *9*(2), 50–66. https://doi.org/10.4319/lom.2011.9.50

Mikelsons, M., & Wang, M. (2018). Interactive online maps make satellite ocean data accessible. *Eos*, *99*. https://doi.org/10.1029/2018eo096563

Qi, L., & Hu, C. (2021). To what extent can Ulva and *Sargassum* be detected and separated in satellite imagery? *Harmful Algae*, *103*, 102001. https://doi.org/10.1016/j.hal.2021.102001

Qi, L., Hu, C., Xing, Q., & Shang, S. (2016). Long-term trend of Ulva prolifera blooms in the western Yellow Sea. *Harmful Algae*, *58*, 35–44. https://doi.org/10.1016/j.hal.2016.07.004

Roelfsema, C. M., Phinn, S. R., Dennison, W. C., Dekker, A. G., & Brando, V. E. (2006). Monitoring toxic cyanobacteria Lyngbya majuscula (Gomont) in Moreton Bay, Australia by integrating satellite image data and field mapping. *Harmful Algae*, *5*(1), 46–56. https://doi.org/10.1016/j.hal.2005.05.001

Sanderson, J. C. (1997). *Subtidal macroalgal assemblages in temperate Australian coastal waters, Australia: State of the environment technical paper series (estuaries and the sea)*. Department of the Environment. Retrieved from https://www.researchgate.net/profile/J-Sanderson/publication/236688368_Subtidal_Macroalgal_Assemblages_in_Temperate_Australian_Coastal_Water/links/0deec532ba8270e29e000000/Subtidal-Macroalgal-Assemblages-in-Temperate-Australian-Coastal-Water.pdf

Soja-Wozniak, M., Darecki, M., Wojtasiewicz, B., & Bradtke, K. (2018). Laboratory measurements of remote sensing reflectance of selected phytoplankton species from the Baltic Sea. *Ocenaologia*, *60*(1), 86–96. https://doi.org/10.1016/j.oceano.2017.08.001

Wen, Q., Jiang, K., Wang, W., Liu, Q., Guo, Q., Li, L., & Wang, P. (2019). Automatic building extraction from Google Earth images under complex backgrounds based on deep instance segmentation network. *Sensors*, *19*(2), 333. https://doi.org/10.3390/s19020333

Zhang, Z., Liu, Q., & Wang, Y. (2018). Road extraction by deep residual u-net. *IEEE Geoscience and Remote Sensing Letters*, *15*(5), 749–753. https://doi.org/10.1109/lgrs.2018.2802944